Attitude Determination&Control System Design for GRACE-like Mission

Neslihan Gülsoy * and Mohaiminul Mesko† and Khady Sarah Sall‡
Istanbul Technical University, Sariyer, Istanbul

Spacecraft Control Systems

UUM532E-22670

Dr. Demet Cilden-Guler

*Graduate Student, Department of Aeronautical& Astronautical Engineering, ID : 511231184
†Graduate Student, Department of Aeronautical& Astronautical Engineering, ID : 511231129
‡Graduate Student, Department of Aeronautical& Astronautical Engineering, ID : 922310129

I. . Introduction

In this report, we delve into the crucial domain of attitude determination and control in the context of space navigation. This exploration stems from the captivating Kelvins competition and is focused on the development of star identification algorithms for star trackers, underscoring the pivotal importance of these technologies for spacecraft navigation and mission success.

The competition at hand aims to refine star identification techniques, which are essential aspects for star trackers deployed aboard spacecraft. These devices play a fundamental role in enabling spacecraft to determine their orientation in space, a critical capability to ensure the success of space missions. The significance of star identification lies in its ability to provide reliable stellar references, enabling navigation systems to maintain precise trajectories and execute manoeuvres with accuracy.

However, the attitude determination and spacecraft control discussed in this report represent complex and crucial challenges. Attitude determination involves determining the spacecraft's orientation relative to a given reference system, an indispensable task for the smooth execution of space operations. Simultaneously, spacecraft control involves implementing systems to maintain or modify this orientation as per the mission's requirements.

In our quest to enhance the efficiency and reliability of spacecraft navigation systems, we rely on filtering the outcomes of star trackers and gyroscope measurement models. Nevertheless, we are aware of potential challenges that may arise in this process. Obstacles such as mathematical model errors, electromagnetic interference, environmental variations, and sensor errors could compromise the accuracy of attitude estimations and disrupt spacecraft control.

In the following sections, we will explore in detail the methods and strategies we plan to adopt to overcome these obstacles and achieve our goals in attitude determination and control.

II. Methodology

The analyzed document, "Attitude Determination and Control System for the GRACE Satellite Mission: Algorithms and Simulation Results," written by Y. Mashtakov et al., [1] provides a comprehensive examination of attitude determination and control systems for the GRACE satellite mission (Gravity Recovery and Climate Experiment). The GRACE mission is crucial for monitoring climate change and understanding terrestrial mass movements, particularly in tracking variations in the Earth's gravitational field.

For our project, this document is essential as it examines several attitude determination and control techniques, thus offering an overview of available approaches. We have chosen to focus on three specific techniques: the Kalman filter, Lyapunov control, and LQR control. In the following lines, we are only giving a brief description of each of them with their governing laws and equations according to the paper. Further in the simulation and Application part, we will dedicate a special part for each of them and will discuss largely them and how we used them to solve our problem.

III. Satellite Dynamics

We get the position of two satellites by doing orbit propagation. The orbital equation of motion is given by:

$$\ddot{\boldsymbol{r}} = \left(-\frac{u}{r^3}\right) \boldsymbol{pos} + \boldsymbol{a}_{\text{dist}}$$

where u is the Earth gravitational constant , r is the radial distance, and $\boldsymbol{r}$ is the position vector. Since $\boldsymbol{a}_{\text{dist}}$ is not considered in orbit propagation, only the first part is considered in the calculations:

$$\ddot{\boldsymbol{r}} = \left(-\frac{u}{r^3}\right) \boldsymbol{r}$$

Then for dynamics calculation, we consider the following right-handed cartesian coordinate systems to derive and model the satellites' dynamics:

- Inertial Frame (IF): The origin is placed at Earth's center of mass. An axis is aligned is with Earth's rotation axis and another one is set in the direction of vernal equinox of the J2000 epoch.
- Orbital Frame (OF): The origin is placed at the satellite's center of mass. The satellite's orbital dynamics dictate the alignment: an axis is parallel to the radius vector but the direction is opposite, and another one is in the opposite- parallel direction to orbital plane normal.
- Body Frame (BF): The satellite's principal axes of inertia dictate the axes system of BF. The first axis is placed at the device line of sight, and another one is normal to the bottom of satellite.
- Reference Frame (RF): This axes system is defined in accordance with the the mission requirements and to keep the line of sight between the two satellites.

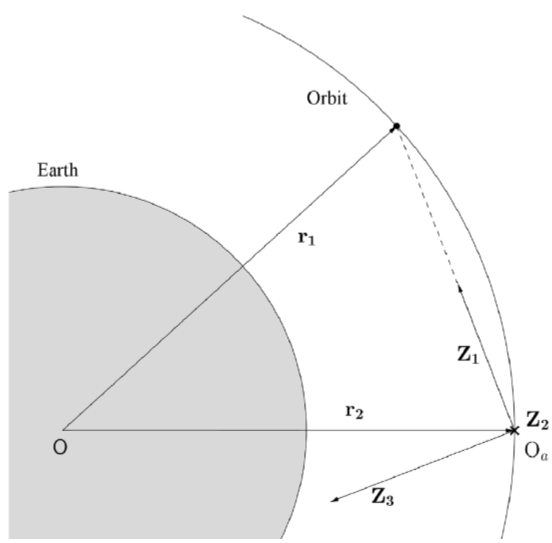

Fig. 1 Reference Frame (RF)

Now, we require to construct the reference frame (RF). We define three orthogonal basis vectors ($\boldsymbol{e_1}$, $\boldsymbol{e_2}$, $\boldsymbol{e_3}$) for the satellite's attitude control and dynamics, and we can calculate them using positions ($\boldsymbol{r}$) and velocities ($\boldsymbol{v}$) of the two satellites. The basis vectors are defined as,

$$\boldsymbol{e_1} = \frac{\|\boldsymbol{r_2} - \boldsymbol{r_1}\|}{\boldsymbol{r_2} - \boldsymbol{r_1}} \qquad \boldsymbol{e}_3 = \frac{\|(\boldsymbol{r}_2 - \boldsymbol{r}_1) \times (\boldsymbol{v}_2 - \boldsymbol{v}_1)\|}{(\boldsymbol{r}_2 - \boldsymbol{r}_1) \times (\boldsymbol{v}_2 - \boldsymbol{v}_1)} \qquad \boldsymbol{e}_2 = \boldsymbol{e}_3 \times \boldsymbol{e}_1 \tag{1}$$

We can calculate the angular velocity of the reference frame (RF), $\boldsymbol{\omega}_{\text{ref}\times}$, with respect to the inertial frame (IF) using D_{ref} as follows:

$$\boldsymbol{\omega}_{\text{ref}\times} = -\dot{\boldsymbol{D}}_{\text{ref}} \boldsymbol{D}_{\text{ref}}^T$$

where

$$\boldsymbol{D}_{\text{ref}} = \begin{bmatrix} \boldsymbol{e}_1^T \\ \boldsymbol{e}_2^T \\ \boldsymbol{e}_3^T \end{bmatrix}$$

The skew-symmetric matrix $\boldsymbol{\omega}_{\text{ref}}\times$ is given by:

$$\boldsymbol{\omega}_{\text{ref}\times} = \begin{bmatrix} 0 & -\omega_{\text{ref},3} & \omega_{\text{ref},2} \\ \omega_{\text{ref},3} & 0 & -\omega_{\text{ref},1} \\ -\omega_{\text{ref},2} & \omega_{\text{ref},1} & 0 \end{bmatrix}$$

The components of the vector $\boldsymbol{\omega}_{\text{ref}}$ are defined as:

$$\omega_{\text{ref},1} = -\frac{1}{2}(e_2 \cdot \dot{e}_3 + \dot{e}_2 \cdot e_3),$$

$$\omega_{\text{ref},2} = -\frac{1}{2}(e_3 \cdot \dot{e}_1 + \dot{e}_3 \cdot e_1),$$

$$\omega_{\text{ref},3} = -\frac{1}{2}(e_1 \cdot \dot{e}_2 + \dot{e}_1 \cdot e_2).$$

To find the derivatives of the vectors $\boldsymbol{e}_1$, $\boldsymbol{e}_3$ and $\boldsymbol{e}_2$ in RF, the following equations are used:

$$\dot{\boldsymbol{e}}_1 = \frac{\boldsymbol{v}_1 - \boldsymbol{v}_2 - \boldsymbol{e}_1 \cdot (\boldsymbol{v}_1 - \boldsymbol{v}_2, \boldsymbol{e}_1)}{\|\boldsymbol{r}_1 - \boldsymbol{r}_2\|} \qquad \dot{\boldsymbol{e}}_3 = \frac{\boldsymbol{h} - \boldsymbol{e}_3(\boldsymbol{h} \cdot \boldsymbol{e}_3)}{\|\boldsymbol{r}_2 - \boldsymbol{e}_1(\boldsymbol{r}_2 \cdot \boldsymbol{e}_1)\|} \qquad \dot{\boldsymbol{e}}_2 = \dot{\boldsymbol{e}}_3 \times \boldsymbol{e}_1 + \boldsymbol{e}_3 \times \dot{\boldsymbol{e}}_1 \tag{2}$$

where $\boldsymbol{h}$ is given by

$$\boldsymbol{h} = \boldsymbol{v}_2 - \boldsymbol{e}_1 \cdot (\boldsymbol{r}_2 - \boldsymbol{e}_1) - \boldsymbol{e}_1 \left[(\boldsymbol{v}_2 \cdot \boldsymbol{e}_1) + (\boldsymbol{r}_2 \cdot \dot{\boldsymbol{e}}_1) \right]$$

Now to calculate the reference angular acceleration ($\dot{\omega}_{\text{ref}}$) , we can assume it as very small or negligible since the satellites are in a nearly stable orbital configuration and move along almost the same orbit. This will help to simplify reducing computational complexity and potential errors in control algorithms.

After discussing spacecraft dynamics in reference frame (RF), next we need to analyze orbital frame (OF) construction and its dynamics. As it is mentioned above the principal axis of inertia is taken as the line of sight of the ranging device. At the same time, the same direction is also an axis of symmetry for the satellite's mass distribution, and this alignment helps reducing the inaccuracies related to satellite's own motion.

We consider the following basis vectors for orbital frame (OF):

$$\boldsymbol{j}_3 = -\frac{\boldsymbol{r}_2}{\|\boldsymbol{r}_2\|}, \qquad \boldsymbol{j}_2 = -\frac{\boldsymbol{r}_2 \times \boldsymbol{v}_2}{\|\boldsymbol{r}_2 \times \boldsymbol{v}_2\|}, \qquad \boldsymbol{j}_1 = \boldsymbol{j}_2 \times \boldsymbol{j}_3. \tag{3}$$

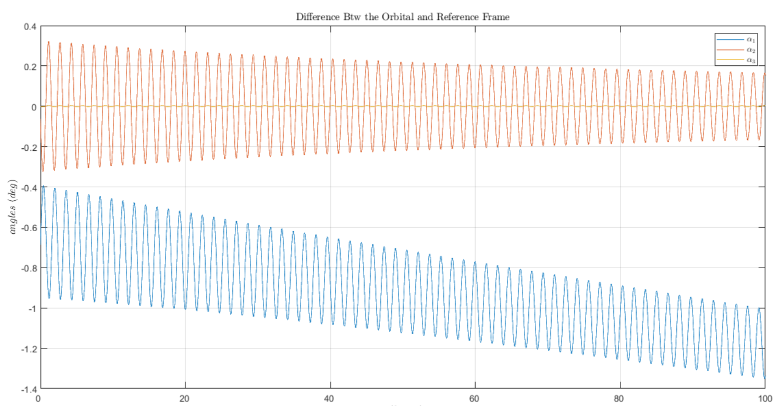

Fig. 2 Difference between the orbital and reference frame

In this project, we implement attitude control laws to have a stabilization according to the Orbital Frame (OF) in its equilibrium point. In this way the satellite will maintain its required orientation to fulfill mission objectives. Further, we can consider the differences between the Orbital Frame (OF) and the Reference Frame (RF) to generate difference between OF and RF in terms of Euler angles $(\alpha_2, \alpha_3, \alpha_1)$ in a specific rotation sequence $2-3-1$.

The Equation of Motion (EoM) for deputy satellite can be written as,

$$\boldsymbol{J}\dot{\boldsymbol{\omega}}_{abs} + \boldsymbol{\omega} \times (\boldsymbol{J}\boldsymbol{\omega}) = \boldsymbol{M}_{ctrl} + \boldsymbol{M}_{ext} \tag{4}$$

where $\boldsymbol{J}$ is the moment of inertia matrix of the satellite, $\boldsymbol{\omega}$ rotation rate of satellite, $\boldsymbol{M}_{ext}$ is torque acting on satellite in body frame and $\boldsymbol{M}_{ctrl}$ is control moment.

$$\dot{\boldsymbol{Q}} = \frac{1}{2}\boldsymbol{Q} \odot \boldsymbol{\omega}_{abs} \tag{5}$$

where $\boldsymbol{Q}$ is the quaternion that describes the transformation from IF to BF. And $\odot$ is quaternion multiplication:

$$\boldsymbol{Q} \odot \boldsymbol{N} = \begin{bmatrix} q_0 \\ \boldsymbol{q} \end{bmatrix} \odot \begin{bmatrix} v_0 \\ \boldsymbol{v} \end{bmatrix} = \begin{bmatrix} q_0 v_0 - (q, v) \\ q_0 \boldsymbol{v} + v_0 \boldsymbol{q} + \boldsymbol{q} \times v \end{bmatrix} \tag{6}$$

The transformation from IF to RF is described by a quaternion, $\boldsymbol{R}$,

$$\dot{\boldsymbol{R}} = \frac{1}{2}\boldsymbol{R} \odot \boldsymbol{\omega}_{ref} \tag{7}$$

The relative angular velocity can be found with,

$$\boldsymbol{\omega}_{rel} = \boldsymbol{\omega}_{abs} - \boldsymbol{S}^{*} \odot \boldsymbol{\omega}_{ref} \odot \boldsymbol{S} \tag{8}$$

where S defines the relative attitude given with $\boldsymbol{S} = \boldsymbol{R}^{*} \odot \boldsymbol{Q}$. The * denotes quaternion conjugation.

To calculate the change of relative angular velocity we Consider the dynamics of $\dot{\omega}_{\text{rel}}$ as follows:

$$\begin{aligned}\dot{\omega}_{\text{rel}} &= \dot{\omega}_{\text{abs}} + \frac{1}{2}\omega_{\text{rel}} \circ S^{\star} \circ S - \frac{1}{2}S^{\star} \circ \omega_{\text{ref}} \circ S \circ \omega_{\text{rel}} - S^{\star} \circ \dot{\omega}_{\text{ref}} \circ S \\ &= \dot{\omega}_{\text{abs}} + \omega_{\text{rel}} \times (S^{\star} \circ \omega_{\text{ref}} \circ S) - S^{\star} \circ \dot{\omega}_{\text{ref}} \circ S\end{aligned}$$

IV. Attitude Control of Satellite

A. Lyapunov based Control

Lyapunov control is a nonlinear control method based on the stability of dynamic systems. In the document's context, Lyapunov control is used to regulate the satellite's attitude using control laws derived from Lyapunov theory. The equations associated with Lyapunov control include:

The Lyapunov equation:

$$V(x) = x^T P x$$

where $V(x)$ is a positive definite Lyapunov function, x is the system state, and P is a positive definite matrix.

The control law derived from the time derivative of $V(x)$:

$$u(t) = -K\frac{\partial V}{\partial x}$$

where $u(t)$ is the control command, K is a control gain matrix, and $\frac{\partial V}{\partial x}$ is the gradient of the Lyapunov function with respect to the system state.

The stability equations derived from Lyapunov theory take the following general form:

$$\dot{V}(x) = \frac{dV}{dt} = \frac{\partial V}{\partial x} \cdot \frac{dx}{dt} = \frac{\partial V}{\partial x} \cdot f(x,u)$$

where: $\dot{V}(x)$ is the time derivative of the Lyapunov function, $\frac{\partial V}{\partial x}$ is the gradient of the Lyapunov function with respect to the system state, $f(x,u)$ is the vector function defining the system's motion.

To demonstrate stability, we aim to show that $\dot{V}(x)$ is negative or zero along the system's trajectories, ensuring that the Lyapunov function decreases or remains constant over time. If $\dot{V}(x)$ is strictly negative, it indicates asymptotic convergence to a stable equilibrium point.

In the context of the studied document, stability equations derived from Lyapunov theory are used to analyze the control system's convergence to a desired equilibrium state, ensuring that control laws derived from the Lyapunov function effectively stabilize the system under varied dynamic conditions.

The Lyapunov-candidate function is chosen as follows Ref.[1],

$$V = \frac{1}{2}(\boldsymbol{\omega}_{rel}, \boldsymbol{J}\boldsymbol{\omega}_{rel}) + k_s(1 - s_0) \tag{9}$$

and the derivative,

$$\dot{V} = (\boldsymbol{\omega}_{rel}\boldsymbol{J}\dot{\boldsymbol{\omega}}_{abs} + \boldsymbol{J}\boldsymbol{\omega}_{rel} \times \boldsymbol{\omega}_{ref}^{BF} - \boldsymbol{J}\dot{\boldsymbol{\omega}}_{ref}^{BF} + k_s\boldsymbol{s}) \tag{10}$$

1. Control Torque generated by Magnetorquers

Magnetorquers are used to generate control torques by using its magnetic fields to have an interaction with the Earth's magnetic field. and therefore the applied torque can change the satellite's attitude. Because of magnetorquers' simple implementation process and low fuel cost requirement, it can be a powerful choice of control. But, due to law of magnetism, it fails to produce control torque in a parallel direction of magnetic field. The control torque generated by the magnetorquers is given by the following:

$$\vec{M}_{\text{ctrl}} = \vec{m} \times \vec{B}$$

Here, $\vec{M}_{\text{ctrl}}$ is the control torque generated,$\vec{m}$ is the magnetic dipole vector produced by the magnetorquers, and $\vec{B}$ is the external magnetic field. We used a simple magnetic field model given at Ref.[1].

$$\boldsymbol{B}^{OF} = \frac{\mu_E}{r^3}\left[\cos u \sin i, \quad -\cos i, \quad 2 \sin u \sin i\right]^T \tag{11}$$

where $\mu_E = 7.812 \times 10^{15}\ m.kg.s^{-2}.A^{-1}$, i is orbit inclination which is 89° for GRACE and u is latitude argument $u = \omega_0 t + u_0$. The ω_0 is orbit angular velocity and it's calculated as 0.0011 rad/sec and t is time.

In the paper, it is discussed that the use of Proportional-Derivative (PD) controllers for magnetorquers can give a better approximation of the desired control actions.The magnetic dipole vector, $\vec{m}$, in this paper is given as follows:

$$\vec{m} = \vec{B} \times (-k_p \vec{s} - k_d \vec{\omega}_{\text{rel}})$$

Here,k_p and k_d are the proportional and derivative gains, respectively, $\vec{s}$ usually represents error in (position error), and $\vec{\omega}_{\text{rel}}$ is the relative angular velocity (rate error).$\vec{m}$ change its orientation according to its present orientation and errors.

The paper suggests to use the following equation for an advanced selection of the magnetic dipole $\vec{m}$,

$$\vec{m} = \frac{1}{B^2}\vec{B} \times \vec{M}_{\text{id}}$$

Here, $\vec{M}_{\text{id}}$ controller's desired ideal torque given with[1];

$$\vec{M}_{\text{id}} = \vec{\omega}_{abs} \times \vec{J}\vec{\omega}_{abs} - \vec{M}_{ext} - \vec{J}[\vec{\omega}_{rel} \times \vec{\omega}^{BF}_{ref}] + \vec{J}\dot{\vec{\omega}}^{BF}_{ref} - k_s \vec{s} - k_w \vec{\omega}_{rel} \tag{12}$$

and $\vec{B}$ is magnetic field vector.

An unit vector $\vec{e}_B$ is defined in the direction of $\vec{B}$, such as:

$$\vec{e}_B = \frac{\vec{B}}{\sqrt{\vec{B} \cdot \vec{B}}}$$

Then, the generated torque $\vec{M}_{\text{gen}}$ can be given as:

$$\vec{M}_{\text{gen}} = \vec{M}_{\text{id}} - \vec{e}_B \left(\vec{e}_B \cdot \vec{M}_{\text{id}}\right)$$

This equation suggests that $\vec{M}_{\text{gen}}$ is the component of $\vec{M}_{\text{id}}$, and which is normal to $\vec{B}$. This effectively nullify the parallel component.

B. Linear Quadratic Regulator

LQR (Linear Quadratic Regulator) control is an optimal control method for linear systems with the purpose of minimizing the quadratic cost function.This method makes a balance between the inclination to reach a certain state i.e. a specific orientation in space and the required control effort to do so.The cost function J in the LQR is given as follows:

$$J = \int_0^{T_f} \left(\vec{x}^T(t)\vec{Q}\vec{x}(t) + \vec{u}^T(t)\vec{R}\vec{u}(t) \right) \, dt + \vec{x}^T(T_f)\vec{P}_f\vec{x}(T_f)$$

where:

- $\vec{x}(t)$:It is the state vector of the system at time t.
- $\vec{u}(t)$: It is the control input applied at time t. The control input in this paper is cosidered as magnetic diapole,$\vec{m}$.
- $\vec{Q}$:It is the state cost matrix.
- $\vec{R}$: It is the control cost matrix.
- $\vec{P}_f$: It is the final state cost matrix for the final time T_f.

The control input is given as:

$$\vec{u}(t) = -\vec{R}^{-1}(t)\vec{B}_{\text{ctrl}}^T(t)\vec{P}(t)\vec{x}(t)$$

The control input for an LQR system for a feedback gain matrix can also be expressed as:

$$\vec{u}(t) = -\vec{K}(t)\vec{x}(t)$$

where the feedback gain matrix $\vec{K}(t)$ is defined as:

$$\vec{K}(t) = \vec{R}^{-1}(t)\vec{B}_{\text{ctrl}}^T(t)\vec{P}(t)$$

The dynamics and control matrices for this project are considered as follows:

$$\boldsymbol{A} = \begin{pmatrix} 0_3 & I_3 \\ A_\alpha & A_\omega \end{pmatrix}$$

$$\boldsymbol{B}_{\text{ctrl}} = \left(0_3 - J^{-1}[\boldsymbol{B}]_\times \right)$$

From the Floquet analysis of controlled relative motion A_α and A_ω are defined as:

$$A_\alpha = \begin{bmatrix} 4\omega_0^2 \frac{C-B}{A} & 0 & 0 \\ 0 & 3\omega_0^2 \frac{C-A}{B} & 0 \\ 0 & 0 & \omega_0^2 \frac{A-B}{C} \end{bmatrix}$$

$$A_\omega = \begin{bmatrix} 0 & 0 & \omega_0 \frac{C+A-B}{A} \\ 0 & 0 & 0 \\ \omega_0 \frac{B-C-A}{C} & 0 & 0 \end{bmatrix}$$

Here the varying state space system can be expressed as:

$$\dot{x} = Ax + Bu$$

where $\dot{x}$ is the time derivative of the system state, A and B are linear system matrices.

The Riccati equations to determine the optimal gain matrix K:

$$A^T P + PA - (PB + KC)^T R^{-1} (PB + KC) + Q = 0$$

here $P(t)$ is found which is used to calculate $K(t)$

These equations describe the process of LQR control to minimize the quadratic cost function by adjusting the control input

After obtaining varying gain matrix $K(t)$ using lqr, a feedback loop is used to varying state space to change the attitude of spacecraft.

LQR is applied to a linearized equation which is obtained from the Floquet analysis of controlled relative motion as well. The following equations are considered for this:

$$\dot{\alpha} = \omega$$

$$\dot{\omega} = \boldsymbol{A}_\alpha \alpha + \boldsymbol{A}_\omega \omega + \boldsymbol{J}^{-1} \left([\boldsymbol{e}_\mathrm{B}^\mathrm{OF}]_\times [\boldsymbol{e}_\mathrm{B}^\mathrm{OF}]_\times \right) (\boldsymbol{J} \boldsymbol{A}_\alpha \omega + \boldsymbol{k}_\alpha \alpha + \boldsymbol{k}_\omega \omega)$$

Here α represent the Euler angles, and the inertia tensor $\boldsymbol{J}$ of the satellite is defined as a diagonal matrix:

$$\boldsymbol{J} = \mathrm{diag}(A, B, C)$$

where A, B, and C are the principal moments of inertia of the satellite.

V. Attitude Determination

Attitude determination with high accuracy is vital to stabilize the satellites. In this paper, the attitude and angular velocity are measured by star trackers and gyroscopes. Since a sensor provides noisy measurements, the accuracy of measurements should be increased using sophisticated methods, like Multiplicative Extended Kalman Filtering (MEKF). By fusing star tracker data with gyro measurements, the MEKF algorithm enhances the robustness and reliability of attitude determination. In this section, first, mathematical models for quaternion measurements by star trackers and gyro measurements will be explained. Then the application of MEKF for the case will be discussed.

A. Star Trackers Modelling and Quaternion Measurement

Star trackers are sophisticated devices used in spacecraft to determine their attitude in space by observing stars. Star tracker directly provides attitude information as quaternion by comparing sensor data with a Star Catalog regarding light intensity and radiation spectrum. For that, at least 2 stars must be in the sensor's field of view (FoV). It needs a priori knowledge of approximate attitude to give more accurate orientation easily in tracking mode.

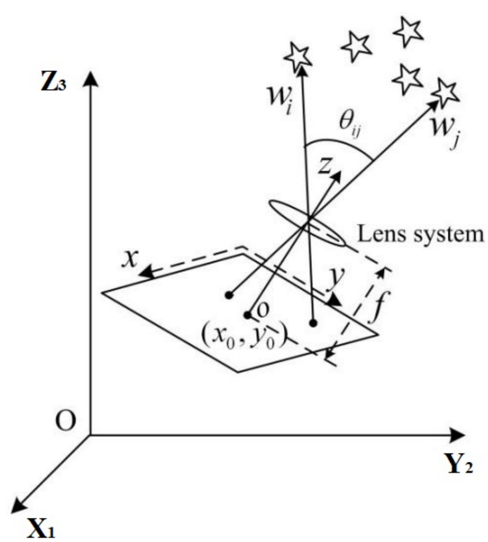

Fig. 3 Measurement model of star tracker

r and ***b*** represent the star vectors in the inertial and the unit star vector in the star tracker frame. And ***M*** is the transformation matrix from inertial frame to body frame. In this study, it is assumed that the reference frame of the star tracker is aligned with the body frame.

The observation of star trackers can be reconstructed in unit vector form as [2],

$$\boldsymbol{b} = \boldsymbol{M}\boldsymbol{r}, \tag{13}$$

where

$$\boldsymbol{b} = \frac{1}{\sqrt{(x - x_0^2) + (y - y_0)^2 + (z - z_0)^2}} \begin{bmatrix} -(x - x_0) \\ -(y - y_0) \\ f \end{bmatrix}, \tag{14}$$

$$\boldsymbol{r} = \begin{bmatrix} \cos\alpha\cos\delta \\ \sin\alpha\cos\delta \\ \sin\delta \end{bmatrix} \tag{15}$$

where f represents the focal length of the star tracker camera and $(x0, y0)$ is the intersection point position of the boresight on the detector plane. (x, y) represents the observed star location on the detector plane. α and δ are the right ascension and declination of the associated guide star on the celestial sphere.

When measurement noise is present, the measurement model becomes,

$$\tilde{\boldsymbol{b}}_i = \boldsymbol{A}\boldsymbol{r}_i + \boldsymbol{v}_i, \quad i = 1, 2, \ldots, N \tag{16}$$

where b_i donates the ith measurement and $\boldsymbol{v}_i$ is the sensor error that can be modelled as Gaussian white noise.

Hipparcos Catalogue is used to obtain star vectors in the inertial frame. The 9th and 10th columns of the catalogue represent the right ascension and declination of stars [3]. In this study, 4 brightest stars (Sirius, Canopus, Rigil Kent, Arcturus) are chosen to track, and their catalogue numbers are 32349, 30438, 71683, and 69673 respectively [4].

After unit star vectors in the inertial frame by Eq. (15), measured star vectors are obtained by Eq. (16) with the true attitude matrix from inertial to the body frame. The sensor error is modelled as Gaussian white noise with a standard deviation of $\boldsymbol{\sigma}_s = \begin{bmatrix} 5 & 5 & 40 \end{bmatrix}^T$ arcsec. Since the quaternion measurement is not provided by star trackers directly, to find additional attitude determination method should be applied to produce observed attitude which is necessary for MEKF.

Davenport's q-method is used for quaternion measurement from star observations because of familiarity with the algorithm.

1. Quaternion Measurement

Wahba problem is given with [5],

$$\text{Minimize} \qquad L(M) = \frac{1}{2}\sum_{i=1}^{N} a_i |\boldsymbol{b}_i - M\boldsymbol{r}_i|^2 \tag{17}$$

such that

$$M^T M = 1$$

where $L(M)$ is the cost, or loss, function and a_i are non-negative weight of i^{th} measurement. Often the weights are chosen as $a_i = 1/\sigma_i^2$. Davenport's q method can be derived as [6]. After some algebraic manipulation, Eq. (17) can be written in a very convenient form as,

$$L(M) = \lambda_0 - tr(M\,B^T) \tag{18}$$

where λ_0 is sum of weights and B is 3×3 attitude profile matrix.

$$\lambda_0 = \sum_{i=1}^{N} a_i \tag{19}$$

$$B = \sum_{i=1}^{N} a_i \boldsymbol{b}_i \boldsymbol{r}_i^T \tag{20}$$

To minimize the loss function, $tr(M\,B^T)$ must be maximized. If quaternion is used, Eq. (18) can be written again as

$$tr(M\,B^T) = q^T K q \tag{21}$$

$$L(M(q) = \lambda_0 - q^T K(B) q \tag{22}$$

$$K(B) = \begin{bmatrix} B + B^T - tr(B) I_{3\times 3} & \boldsymbol{z} \\ \boldsymbol{z}^T & tr(B) \end{bmatrix} \tag{23}$$

$$\boldsymbol{z} = \begin{bmatrix} B_{23} - B_{32} \\ B_{31} - B_{13} \\ B_{12} - B_{21} \end{bmatrix} = \sum_{i=1}^{N} a_i (\boldsymbol{b}_i \times \boldsymbol{r}_i) \tag{24}$$

where $K(B)$ is 4×4 a symmetric trace-less matrix. q method asserts that the eigenvector of K matrix gives optimal quaternion, so it gives the best estimate of the orientation matrix.

$$Kq_{opt.} = \lambda_{max} q_{opt.} \tag{25}$$

$$L(\hat{A}(q_{opt.})) = \lambda_0 - \lambda_{max} \tag{26}$$

B. Gyro Measurement Modelling

The Gyro measurement model in the body frame with respect to the inertial frame can be given as,

$$\tilde{\omega}_b = \boldsymbol{\omega} + \eta_g + \boldsymbol{b_g} \tag{27}$$

where $\boldsymbol{\omega}$ is the true angular velocity derived with EoM, $\boldsymbol{b_g}$ is the gyro bias vector and η_g is the sensor error of gyros.

In this project, bias is not considered and sensor errors are taken as zero mean Gaussian white noise with standard deviations of $\sigma_w = \begin{bmatrix} 0.006 & 0.006 & 0.006 \end{bmatrix}^T rad/sec.$

C. Kalman Filtering

Using the star trackers and gyro measurements without filtering can affect the control system's performance. Because of that, the Multiplicative Kalman Filter (MEKF) is applied. The MEKF formulations following the Ref. [7] are shown below

The error quaternion is described by [7],

$$\delta \boldsymbol{q} = \boldsymbol{q} \otimes \hat{\boldsymbol{q}}^{-1} \tag{28}$$

where $\hat{\boldsymbol{q}}$ is the estimated quaternion and the derivative of error quaternion is,

$$\delta \boldsymbol{q} = \dot{\boldsymbol{q}} \otimes \hat{\boldsymbol{q}}^{-1} + \boldsymbol{q} \otimes \dot{\hat{\boldsymbol{q}}}^{-1} \tag{29}$$

Also, it can be written as,

$$\delta \dot{\boldsymbol{q}} = -\begin{bmatrix} [\hat{\omega}_x]\delta \boldsymbol{q}_{1:3} \\ 0 \end{bmatrix} + \frac{1}{2}\begin{bmatrix} \delta\omega \\ 0 \end{bmatrix} \otimes \delta \boldsymbol{q} \tag{30}$$

With the above equations, with first and second-order approximations, the linearized equation for quaternion error is,

$$\delta \dot{\boldsymbol{q}}_{1:3} = -[\hat{\omega}_X]\delta \boldsymbol{q}_{\boldsymbol{1:3}} + \frac{1}{2}\delta\omega \tag{31}$$

$$\delta \dot{q}_4 = 0 \tag{32}$$

The small angle approximation lead to $\delta\dot{\boldsymbol{q}}_{1:3} = \delta\boldsymbol{\alpha}_2$, where $\delta\boldsymbol{\alpha}$ contains Euler angles errors. Also the error angular velocity is given with

$$\delta\omega = \omega - \hat{\omega} \tag{33}$$

If the states for kth iteration are chosen as $\Delta\boldsymbol{x} = \begin{bmatrix} \delta\boldsymbol{\alpha}^T & \delta\boldsymbol{\omega}^T \end{bmatrix}^T$, the MEKF error model becomes,

$$\Delta\dot{\boldsymbol{x}}_k = \boldsymbol{F}_k\Delta\boldsymbol{x}_k + G_k\boldsymbol{w}_k \tag{34}$$

where the linearized transition matrix F considering the external moment is given as [1],

$$\boldsymbol{F} = \begin{bmatrix} -[\hat{\omega}_k\times] & 0.5\boldsymbol{I}_{3\times3} \\ 6\frac{\mu_E}{r^5}([\hat{\boldsymbol{D}}\boldsymbol{r}]_X\boldsymbol{J}[\hat{\boldsymbol{D}}\boldsymbol{r}]_X - [\boldsymbol{J}\hat{\boldsymbol{D}}\boldsymbol{r}]_X[\hat{\boldsymbol{D}}_k\boldsymbol{r}]_X) & [\boldsymbol{J}\hat{\omega}_X] - [\hat{\omega}]_X\boldsymbol{J} \end{bmatrix} \tag{35}$$

where $\hat{\boldsymbol{D}}$ is the estimated attitude matrix. The current expected error is described by the covariance matrix $\boldsymbol{P}$ is used,

$$\dot{\boldsymbol{P}}_k = \boldsymbol{F}_k\boldsymbol{P}_k\boldsymbol{F}^T + \boldsymbol{Q} \tag{36}$$

the state covariance matrix $\boldsymbol{Q}$ is taken as $0.05\boldsymbol{I}_{6\times6}$. After the priori estimation, the estimation for states and the erros should be updated considering the observation.

$$\Delta\hat{\boldsymbol{x}}_k^+ = \boldsymbol{K}_k\,[\tilde{\boldsymbol{y}}_k - \boldsymbol{h}_k(\hat{\boldsymbol{x}_k}^-)] \tag{37}$$

where $\tilde{\boldsymbol{y}}$ contains the measurement from star trackers and gyroscopes, and $\boldsymbol{h}$ is the nonlinear observation matrix. And the Kalman gain, $\boldsymbol{K}$ is calculated with,

$$\boldsymbol{K}_k = \boldsymbol{P}_k^-\boldsymbol{H}_k^T\left[\boldsymbol{H}_k\boldsymbol{P}_k^-\boldsymbol{H}_k^T + \boldsymbol{R}_k\right]^{-1} \tag{38}$$

where the $\boldsymbol{H}$ is linearized observation matrix, $\boldsymbol{R}$ is the covariance matrix of observations. Also, the estimated covariance matrix should be updated as,

$$\boldsymbol{P}_k^+ = [\boldsymbol{I} - \boldsymbol{K}_k\boldsymbol{H}_k]\,\boldsymbol{P}_k^- \tag{39}$$

The updated quaternion and angular velocity estimations are,

$$\hat{\boldsymbol{q}}_k^+ = \hat{\boldsymbol{q}}_k^- + \frac{1}{2}\Xi(\hat{\boldsymbol{q}}_k^-)\delta\alpha_k^+ \tag{40}$$

$$\hat{\omega}^{+} = \omega_k^{-} + \delta\hat{\omega}_k^{+} \tag{41}$$

where $\Xi(\hat{\boldsymbol{q}})$ is,

$$\Xi(\hat{\boldsymbol{q}}) = \begin{bmatrix} q_4 \boldsymbol{I}_{3\times3} + [\boldsymbol{q}_{1:3}]_X \\ -\boldsymbol{q}^T \end{bmatrix} \tag{42}$$

since the measured quaternion is used directly, the linearized observation matrix,

$$\boldsymbol{H} = \boldsymbol{I}_{6\times6} \tag{43}$$

Also, the covariance matrix is taken as $\boldsymbol{R} = diag(21.2848^2 \boldsymbol{I}_3, 0.006^2, 0.006^2, 0.006^2))$

VI. Result and Discussion

A simulation in Simulink environment is done with a fixed step size of 10 seconds for 10 hours. The positions of satellites are generated by orbit propagation. The results from orbit propagation are used to generate the gravity gradient torques and magnetic field in orbit frame.

A. Satellite Dynamics Analysis

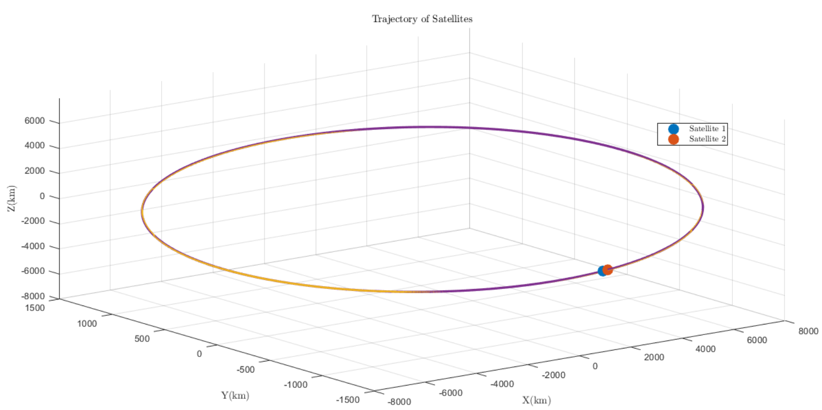

Fig. 4 Orbit of two satellites

The orbits of satellites are shown in Fig.(**??**). And the Gravity Gradient torque acting on the deputy satellite is shown at Fig.(5).

By doing orbital propagation, we get the trajectory of two satellites. It can be seen from the figure that they rotate around the same orbit as discussed previously.

This plot given information on oscillation of the torque over time. It helps to find the natural frequencies of the system. Since in this plot the graph shows periodic oscillations, the spacecraft system can be considered marginally stable. Gravity gradient (GG) torques are the cause of satellite's orientation changing, so to make a satellite point to a

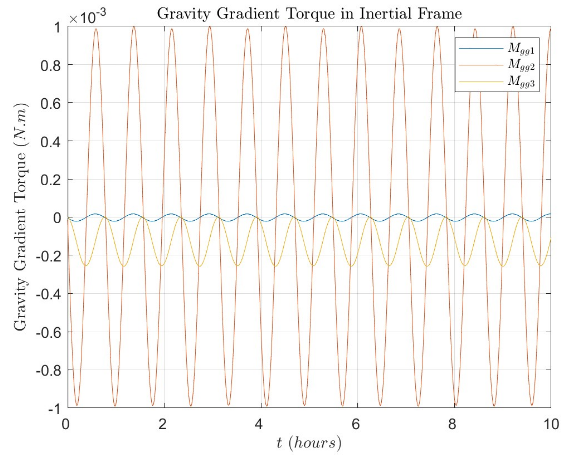

Fig. 5 Gravity Gradient Torque in Orbit Frame

direction requires control effort. Here, the GG torque is observed to be quite high due to the large moment of inertia.

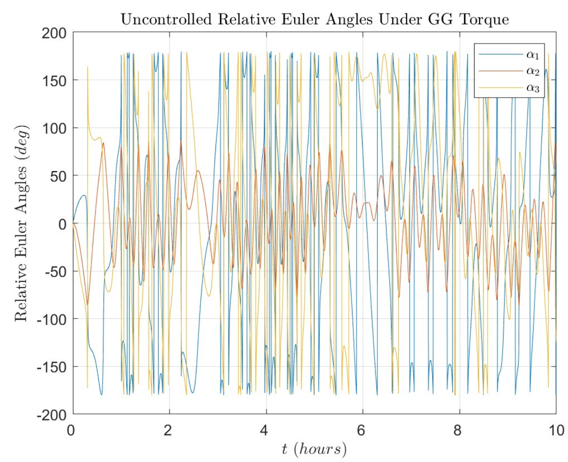

Fig. 6 Uncontrolled Relative Euler Angles under GG over time

In this figure, it can be observed how the relative Euler angles change over time under GG torque. Relative Euler angle is mainly the relative Euler angle of deputy satellite with respect to the leader satellite. Now to orient the deputy spacecraft to a particular direction will require some sort of control device, such as magnetorquers to match the Euler angle of deputy satellite.

B. Magnetorquers and LQR Analysis

Here, a plot of the magnetic field ($\boldsymbol{B}$) in the orbital frame over time is obtained. It helps to calculate control moment $\boldsymbol{M}_{\text{ctrl}}$, that is desired to be produced by the magnetorquer. To generate $\boldsymbol{M}_{\text{ctrl}}$ for LQR calculation, an additional PD controller is used with coefficients $k_\alpha = \text{diag}([0.0012, 0.0030, 0.0005])$ and $k_\omega = \text{diag}([2.05, 3.5, 0.5])$.

By using the LQR control approach, the required magnetic dipole moment to orient the spacecraft can be found. Its

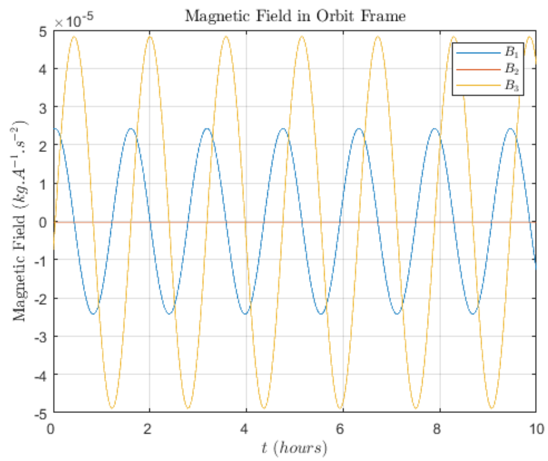

Fig. 7 Magnetic Field in OF over time

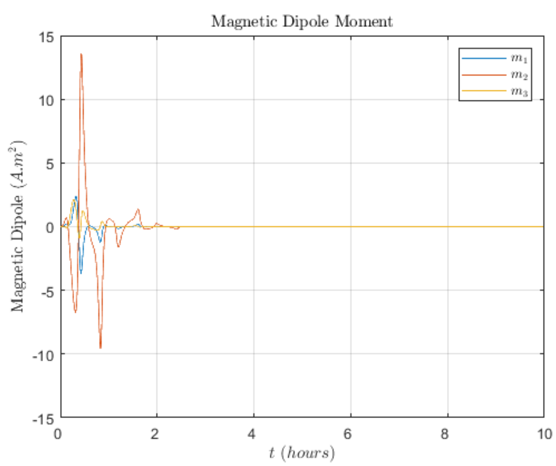

Fig. 8 Magnetic Diapole Moment over time

maximum value is seen as around 13 Am^2. Here, we can see LQR can indicate the amount of current necessary in the magnetorquer coils and also how it should vary according to the magnetic dipole requirement calculation done by this approach. Additionally, by using the Q and R cost matrices of LQR, we can optimize the energy usage of magnetorquers. In this figure, we can see how the Relative angular velocity (ω_{rel}) changes with time. With the use of LQR, the second

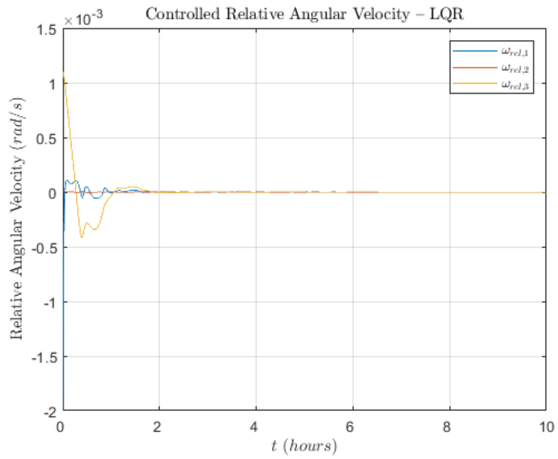

Fig. 9 Relative Angular Velocity controlled using LQR over time

spacecraft's relative angular velocity becomes zero with the transient time of 1.7411 hours. That means the angular velocities of the two satellites become the same and it implies that they spin at the same rate.

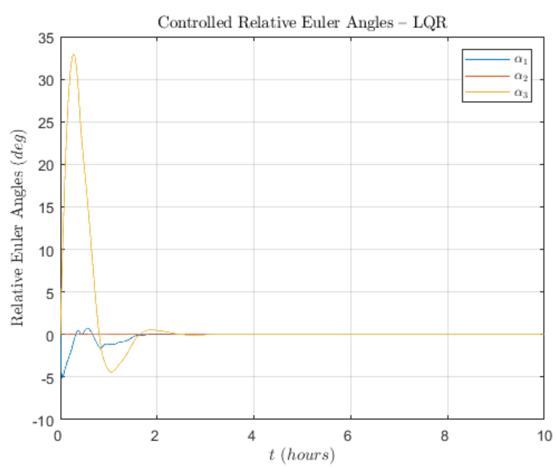

Fig. 10 Relative Euler Angles controlled over time

Here in this figure, we can see after applying LQR, the relative Euler angles go to zero degrees with a transient time of 1.6955 hours. This implies that the orientation of the second spacecraft becomes the same as the leader satellite. It happens as Ω_{rel} approaches zero. Therefore, we have been able to obtain stability for this spacecraft.

We have done the control calculation assuming low control requirement. This is why only magnetorquer is used to control the satellite. However, in reality, thrusters are also needed to control a heavy satellite with big mass.

C. Attiude Estimation

A MEKF is designed for the attitude estimation of the deputy. The parameters are mentioned at Sec.(V). First, the quaternion measurement is done with Davenport's q-method with star vector measurement model explained in Sec.(V.A). Also, the gyroscope measurements are generated as given in Eq.(27) without the bias term. Then, the equations for MEKF were adapted to the Simulink by following the formulation given Sec.(V.C). The designed filter is used to estimate the angular velocity of deputy satellite in body frame with respect to inertial frame as well as the quaternions defining the transition from inertial frame to body frame. The results are generated under Lyapunov-based controlled satellite.

RMSE	Measured States	Filtered States
α $(arcsec)$	17.2042	7.9657
ω $(arcsec/sec)$	1228	6.3492e-7

Table 1 RMSE Values for Measured and Filtered States

The differences between the true states and estimated and measured states are calculated within simulation time. The results are shown below. When Figs.[(11) - (12)] are considered together, it can be seen that the filter greatly increases the accuracy for both Euler angles and angular velocity. The Root-mean-square error (RMSE) values for both measured states and filtered measurements are calculated and shown at Tab.(1).

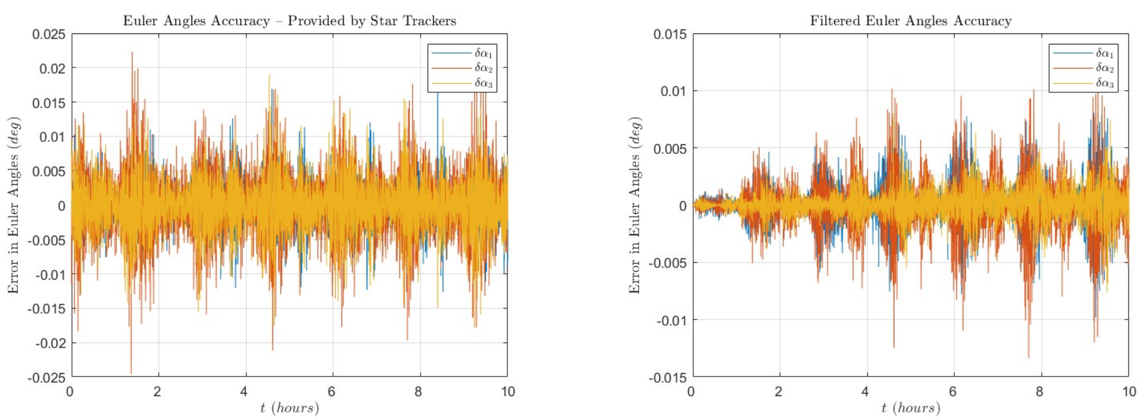

(a) Accuracy of Quaternion Measurement Model **(b) Accuracy of Filtered Attitude Measurement**

Fig. 11 Accuracy of Quaterninon Measurement Model and EKF

The filter shows great results, especially for angular velocity measurements. The accuracy in attitude filtering can be increased by tuning the covariance matrices of process and measurement. However, the results found guarantee that the designed filter can be used for the control part.

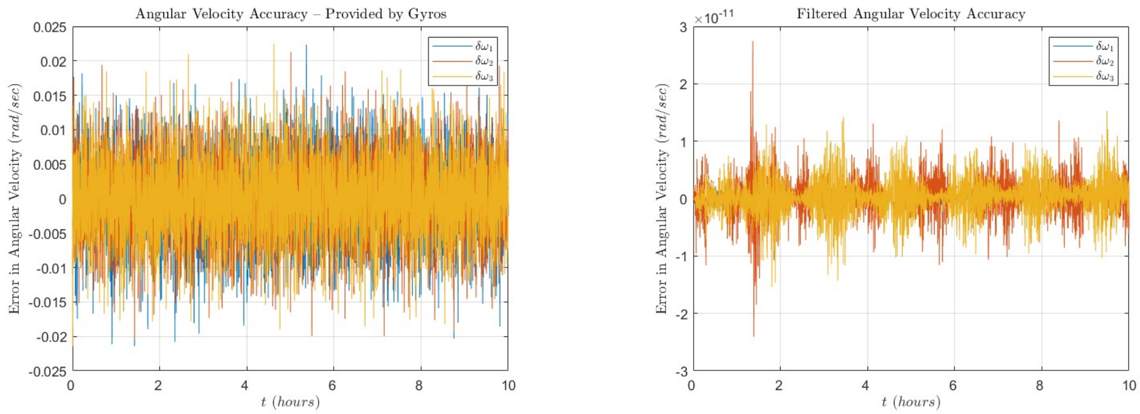

(a) Accuracy of Gyro Measurement Model **(b) Accuracy of Filtered Gyro Measurement**

Fig. 12 Accuracy of Gyro Measurement Model and EKF

D. Attitude Control

1. Lyapunov based control for Stabilization

In our reference paper, we have the control moment generated by the magnetorquers. Instead of re-implementing the Lyapunov control function, we directly used this control moment. Indeed, this control moment stems from the application of Lyapunov-based control, requiring asymptotic stability, meaning that the derivative of our Lyapunov function must be negative. Therefore, we did not re-implement this function but used the control moment as is, providing all the parameters required by its expression, including those related to the magnetic field.

The precise determination of the magnetic field was crucial for this step. We used the IGRF model to obtain the necessary data for this determination, taking into account the satellite's positions. Using this control moment, we directly determined the derivative of the angular velocity. The relationship between the derivative of the angular velocity and the control moment is established in the equation of motion. Using this relationship, we calculated the derivative of the satellite's angular velocity. Then, we integrated this derivative to obtain the effective angular velocity.

From this angular velocity, we implemented a method to obtain a set of controlled quaternions. This set of quaternions allowed us to determine the satellite's attitude by calculating the Direct Cosine Matrix, the true attitude matrix of the satellite. This attitude matrix is stabilized because it is obtained directly from the controlled angular velocity, i.e., the desired angular velocity for the satellite.

This attitude matrix is then used to estimate the satellite's attitude using the Kalman filter, as mentioned earlier. Thus, it is as if, by estimating the satellite's attitude over time, we simultaneously stabilize it using the Lyapunov control that generated the control moment with the help of the magnetorquers. By using this control moment, the process acts as if the attitude were stabilized at the same time as its estimation.

To ensure excellent stabilization of our parameters and consequently of our satellite, we chose the gains k_s =

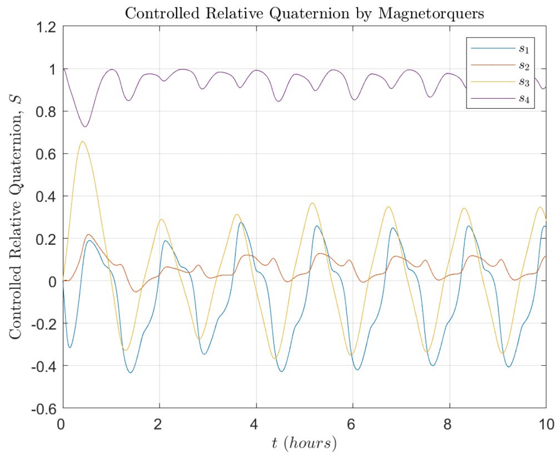

Fig. 13 Magnetorquers-based control of quaternions

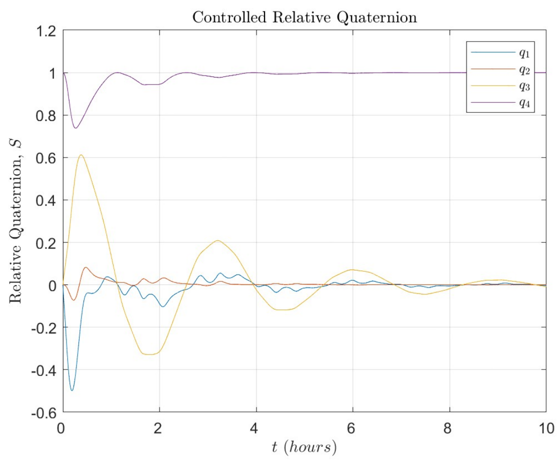

Fig. 14 Lyapunov-based control of Quternions – Ideal Case

$2 * \text{diag}([0.0012; 0.0030; 0.0005])$; $k_w = \text{diag}([2.05; 3.5; 0.5])'$. Initially, we attempted stabilization using only magnetorquers to control the relative quaternions, but noticed imperfect stabilization. All quaternions oscillated around zero, and the scalar quaternion did not reach its assigned value. However, when we tried the Lyapunov-based control with $\vec{M}_{id}$ given at Eq.(12) for quaternions, the stabilization significantly improved. Quaternions all tended towards zero, except the scalar quaternion, which converged to its designated value. The transient time is 3.0578 hours.

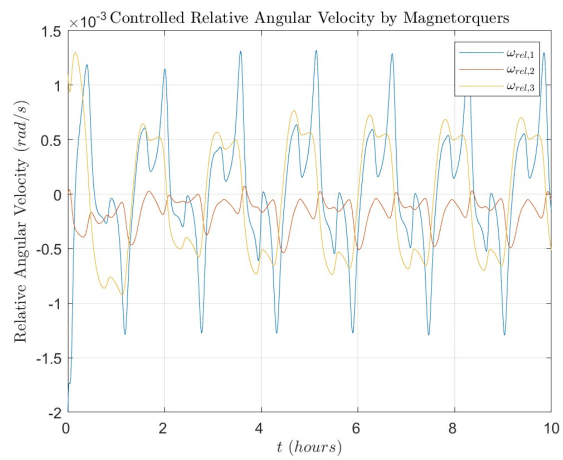

Fig. 15 Magnetorquers based control of relative angular Velocity

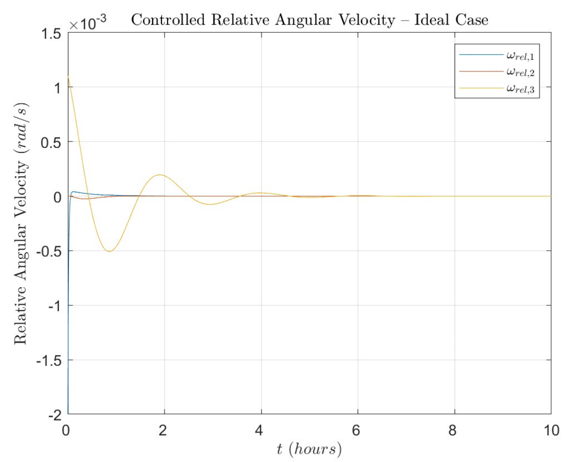

Fig. 16 Lyapunov-based Control of relative angular Velocity – Ideal Case

For controlling angular velocity, shown in Figs.(16,15), we observed similar results. When controlled solely by magnetorquers, we experienced oscillations without notable stabilization. Conversely, with the Lyapunov Based Control, we achieved satisfactory stabilization around zero, meeting our objectives. The transient time is 2.4272 hours.

Regarding relative Euler angles, we found that without controlling under the gravity gradient, we obtained dense oscillations without stabilization. Even with only magnetorquers, we did not achieve convergence to zero, indicating control inefficiency. However, with Lyapunov Basic Control, we observed significant stabilization as shown in Fig.(18).

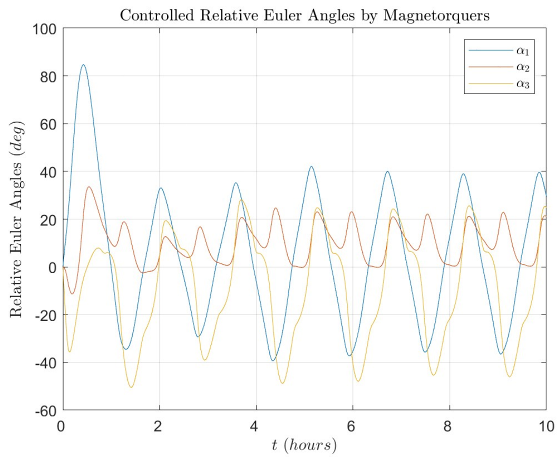

Fig. 17 Magnetorquers-based control of Relative Euler Angles

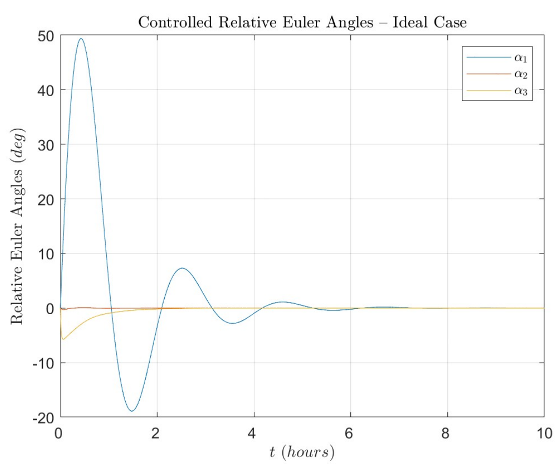

Fig. 18 Lyapunov-based control of Relative Euler Angles – Ideal Case

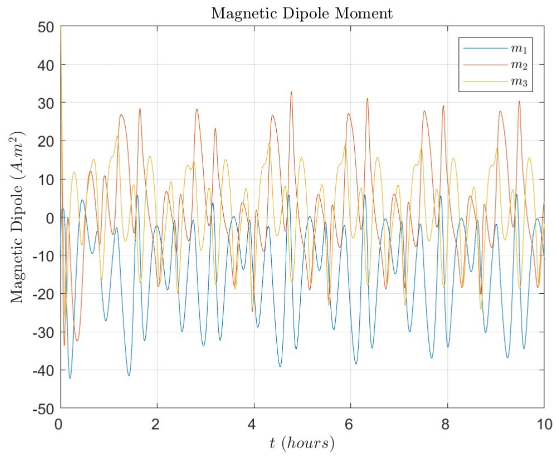

Fig. 19 Lyapunov-based control of Magnetic Dipole Moment

The magnetic dipole moment produced by magnetorquers is shown at Fig.(19).

Possible Explanations:

System Complexity: Attitude control of a satellite is a complex problem due to the nonlinear dynamics of the system, interactions between different parameters, and physical constraints such as gravity and Earth's magnetic field. Control methods must account for this complexity to ensure effective stabilization.

Nature of Commands: Magnetorquers are devices that generate magnetic moments to control the satellite's orientation in response to Earth's magnetic field. However, their exclusive use may not be sufficient to stabilize the system due to their limited nature and ability to control only certain parameters.

Lyapunov Approach: Lyapunov Based Control utilizes principles from stability theory, including Lyapunov functions, to design controllers that guarantee asymptotic stability of the system. This approach allows for analysis of the system's stability as a whole and the design of robust controllers that continuously adjust commands to maintain stability.

Parameter Optimization: The gains used in control methods, such as k_s and k_w, are essential in determining system performance. The values of these gains must be carefully chosen to ensure a stable and fast response while avoiding undesirable oscillations.

Adaptability of Control: Lyapunov-based Based Control acts as a more sophisticated feedback mechanism, capable of continuously adjusting control parameters to adapt to dynamic system variations. This ensures robust performance even in variable and unforeseen conditions.

By combining these factors, we can understand why Lyapunov Based Control yielded superior results compared to the exclusive use of magnetorquers. This approach offers better capability to stabilize the system by considering its complexity and adaptively adjusting commands to achieve and maintain optimal stability. The Lyapunov control acts as a feedback mechanism that continuously adjusts the satellite's orientation to achieve and maintain stability around the desired target as we have seen.

To sum up, we designed the attitude determination and control system for a GRACE-like mission. We propagated the positions of 2 satellites, calculated the gravity-gradient torque acting on the deputy and tried to stabilize the relative motion of the deputy with respect to the leader satellite. As actuators, we only model the magnetorquers. However, it's seen that only magnetic control could not produce the torque necessary to stabilize the satellite and additional control approaches are needed. For LQR-based controlled, additional PD controller feeding the linearized dynamics is designed and acceptable results were achieved compared to Lyapunov-based magnetic control. On the other hand, the designed EKF shows acceptable results for controlled motion, for further analysis, it can be used on uncontrolled motion.

References

[1] Mashtakov, Y., Ovchinnikov, M., Wöske, F., Rievers, B., and List, M., "Attitude determination control system design for gravity recovery missions like GRACE," *Acta Astronautica*, Vol. 173, 2020, pp. 172–182. https://doi.org/10.1016/J.ACTAASTRO.2020.04.019.

[2] Wang, J.-Q., "Autonomous on-orbit calibration of a star tracker camera," *Optical Engineering*, Vol. 50, 2011, p. 023604. https://doi.org/10.1117/1.3542039.

[3] "Catalogues - Hipparcos - Cosmos," , 2024. URL https://www.cosmos.esa.int/web/hipparcos/catalogues.

[4] "The 50 Brightest Stars - Hipparcos - Cosmos," , 2024. URL https://www.cosmos.esa.int/web/hipparcos/brightest.

[5] de Ruiter, A. H., Damaren, C. J., and Forbes, J. R., *Spacecraft Dynamics and Control: An Introduction*, WILEY, 2013.

[6] Markley, L., and Mortari, D., "Quaternion Attitude Estimation Using Vector Observations," *Journal of the Astronautical Sciences*, Vol. 48, 2000, pp. 359–380. https://doi.org/10.1007/BF03546284.

[7] Crassidis, J. L., and Junkins, J. L., *Optimal Estimation of Dynamic Systems, Second Edition (Chapman & Hall/CRC Applied Mathematics & Nonlinear Science)*, 2nd ed., Chapman & Hall/CRC, 2011.